Bespalova, Kristina; Ross, Glenn; Suihkonen, Sami; Paulasto-Kröckel, Mervi

Metalorganic Chemical Vapor Deposition of AlN on High Degree Roughness Vertical Surfaces for MEMS Fabrication

Published in:
Advanced Electronic Materials

DOI:
10.1002/aelm.202300628

Published: 01/04/2024

Document Version
Publisher's PDF, also known as Version of record

Please cite the original version:
Bespalova, K., Ross, G., Suihkonen, S., & Paulasto-Kröckel, M. (2024). Metalorganic Chemical Vapor Deposition of AlN on High Degree Roughness Vertical Surfaces for MEMS Fabrication. *Advanced Electronic Materials*, *10*(4), Article 2300628. https://doi.org/10.1002/aelm.202300628

ADVANCED ELECTRONIC MATERIALS Open Access
www.advelectronicmat.de

Metalorganic Chemical Vapor Deposition of AlN on High Degree Roughness Vertical Surfaces for MEMS Fabrication

Kristina Bespalova, Glenn Ross, Sami Suihkonen, and Mervi Paulasto-Kröckel*

Aluminum nitride (AlN) grown on vertical surfaces can be utilized for the fabrication of advanced piezoelectric microelectromechanical systems (MEMS). The in-plane motion of the parts of a MEMS element is possible when AlN is deposited on the vertical surfaces of the moving structure. For the best device performance, AlN must have high crystal quality, uniform coverage of the vertical sidewalls, and c-axis crystalline orientation perpendicular to the plane of a vertical surface. The impact of the surface roughness (R_q) of the vertical sidewalls formed in Si using wet and dry etching methods on the crystal quality, crystallographic orientation, and uniformity of the metalorganic chemical vapor deposited (MOCVD) AlN thin films is studied in this paper. In both cases, AlN films demonstrated full sidewall coverage and grew crystalline in the c-axis direction. AlN films grown on vertical Si surfaces achieved using anisotropic wet etching are highly crystalline and oriented in [0001] direction, while the films grown on vertical surfaces achieved using dry etching displayed a lower level of alignment with the Si sidewalls.

1. Introduction

Surface micromachining fabrication methods intended for work with planar structures are prevalent and effective for achieving high precision and functionality devices in microelectromechanical systems (MEMS). However, the growing demand for miniature and multifunctional devices requires alternative approaches beyond the traditional surface micromachining, such as the deposition and patterning of high-quality thin films over vertical surfaces. Thus, piezoelectric thin films grown on vertical surfaces provide novel opportunities to sense, harvest, and drive parts of a device in-plane, as well as to combine it with motion in other directions. The approach proposed in the work presents an opportunity to overcome the constraints of conventional designs and unlock alternative paths in device fabrication.

The interest in aluminum nitride (AlN) deposition on vertical surfaces for MEMS application has been growing in the last decade.[1–5] We have recently demonstrated aluminum nitride (AlN) films deposited on vertical Si (111) sidewalls of Si (110) substrates by metalorganic chemical vapor deposition (MOCVD),[1,3] and the fabrication process of the laterally moving actuator on its base.[1] This fabrication principle can be adapted for the design of piezoelectric gyroscopes, harvesters, and micromanipulators that ensure lower power consumption and a smaller area on a chip compared to existing analogs. Such MEMS require the formation of complex structures in Si substrate via etching processes, for example, cantilevers or other geometrical objects, explicitly designed for the deposition of AlN films on their vertical surfaces. Wet etching of Si provides low surface roughness (R_q) of the sidewalls, but such methods are time-consuming. Moreover, as wet etching is an anisotropic process additional unwanted slanted Si (111) surfaces may form during the etching process. Dry etching processes can achieve high etching rates for Si, but normally results in vertical sidewalls with a high degree of surface roughness. Previous research demonstrates that the crystal quality and piezoelectric properties of AlN films depend on the R_q and the crystallographic orientation of the substrate.[6–10] The electric field should be aligned parallel to the c-axis of AlN for the maximum efficiency of the electromechanical coupling and R_q can contribute to the grains tilt. In turn, the crystal quality and orientation of AlN thin films are closely linked to the device performance. For example, the influence of the AlN crystal quality on the resonance frequency of piezoelectric micromachined ultrasonic transducers was demonstrated in the work.[11] Therefore, the etching methods for vertical sidewalls formation in Si and its impact on the crystal quality and orientation of AlN should be extensively studied.

Previously, MOCVD deposited AlN with c-axis texture has been demonstrated on the Si (111) vertical surfaces, formed using etching in potassium hydroxide (KOH).[1] However, KOH is not CMOS compatible due to the presence of alkali metal potassium (K+) ions in it.[12,13] Therefore, other etching solutions should be considered for wet etching of Si. Tetramethylammonium hydroxide (TMAH) is a commonly used etchant in MEMS technology, that is CMOS-compatible and has

K. Bespalova, G. Ross, S. Suihkonen, M. Paulasto-Kröckel
Aalto-yliopisto
Tietotie 3, Espoo 02150, Finland
E-mail: kristina.bespalova@aalto.fi

The ORCID identification number(s) for the author(s) of this article can be found under https://doi.org/10.1002/aelm.202300628

DOI: 10.1002/aelm.202300628

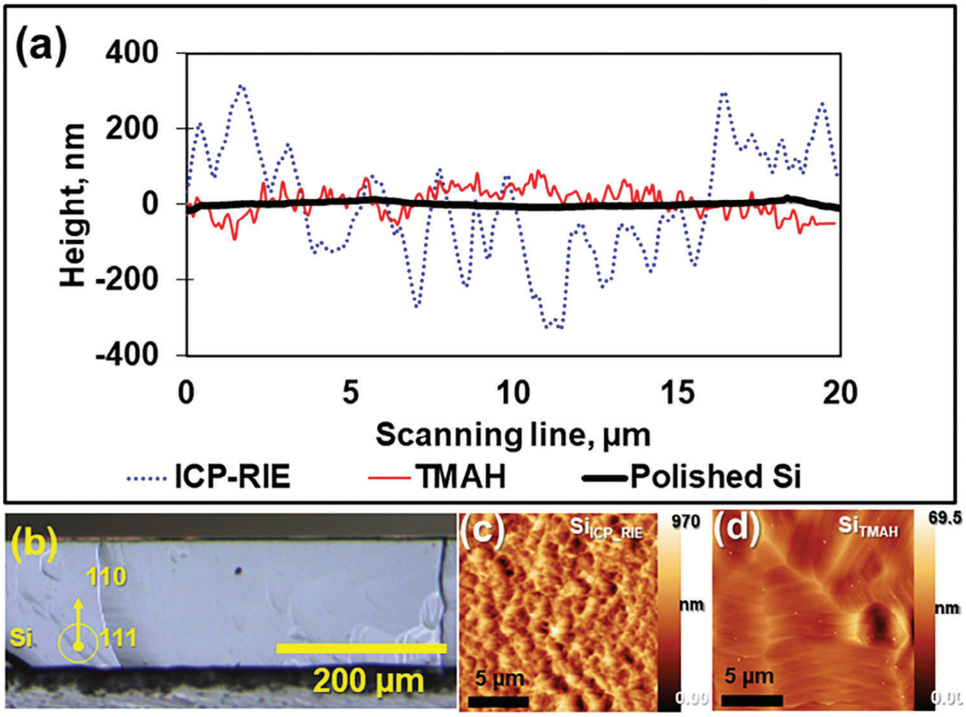

Figure 1. a) Height profiles of vertical Si (111) surfaces achieved using ICP-RIE and TMAH 25% over 20 µm scanning line in comparison to polished Si (111) surface of the blank wafer; b) Vertical Si sidewall achieved by TMAH etching; AFM micrographs of the defects formed in Si (111) vertical sidewalls etched in c) ICP-RIE and d) TMAH. Scanning area was 20 × 20 µm.

excellent selectivity to SiO_2.[14] In this paper, we study Si (111) sidewall formation on Si (110) wafers by TMAH and ICP-RIE and the growth of MOCVD AlN thin films on the formed sidewalls. Sidewall roughness of wet and dry etched vertical sidewalls is characterized and the effect of sidewall R_q on crystalline quality and orientation of MOCVD deposited AlN is analyzed. The correlation between the root mean square (RMS) value of sidewall R_q and mosaicity and crystalline orientation of AlN is observed. Additionally, we investigate the effectiveness of TMAH treatment for the surface smoothing of ICP-RIE etched Si sidewalls.

2. Results and Discussion

2.1. Si (110) Etching and Vertical Si (111) R_q Measurement

Figure 1a shows atomic force microscopy (AFM) linescans of the vertical sidewalls achieved using inductively coupled plasma reactive-ion etching (ICP-RIE) and TMAH 25% solution together with a scan of a blank Si (111) substrate surface. The cavity sidewalls were aligned with Si (111) orientation in Si (110), as shown in Figure 1b.

Table 1 presents measured R_q of the vertical sidewalls on five locations on the wafer. Vertical Si sidewalls formed in Si (110) using ICP-RIE ($Si_{ICP-RIE}$) have a rough surface as was expected. Also, the R_q varies strongly over the wafer. Si (111) vertical sidewalls in Si (110) formed by TMAH etching (Si_{TMAH}) are significantly smoother. R_q of the Si_{TMAH} does not exceed 9 nm, however, 50 nm deep etching pits were observed on these vertical sidewalls in some areas over the wafer (Figure 1d). Etching pits (etch-pits) is a common phenomenon that occurs when using wet etching for Si.[15] The etching pits appear because of the dislocations in Si or contaminating particles in the etching solution. The surface planes of the etch-pits on Si (111) are $\{11\bar{2}\}$ and $\{\bar{1}\bar{1}2\}$ crystallographic families. Thus, AlN crystal growth on the walls of the etching pits is expected to differ from the growth on Si (111). No etch pits were observed on ICP-RIE etched wafers.

Post-dry etching treatment by TMAH was performed on $Si_{ICP-RIE}$. The measured R_q values are summarized in **Table 2**. Post ICP-RIE etching treatment by TMAH can reduce R_q of Si vertical sidewalls by 33–54%. Increasing the TMAH treatment time did not result in increased smoothening of the surface. The smoothening seems to be more related to the initial roughness of the sample and reaches a threshold at around $R_q = 100$ nm, regardless of etching time and initial roughness. However, even after the treatment, the R_q remains high in all samples, and such a method is not effective for smoothening of high roughness sidewall surfaces generated by ICP-RIE.

Table 1. R_q of vertical Si sidewalls achieved using dry and wet etching.

Place on the wafer	R_q, nm (ICP-RIE)	R_q, nm (TMAH, 70 °C, 25%)
N	217.2 ± 6.7	2.0 ± 0.1
W	157.0 ± 3.0	4.5 ± 0.1
E	241.7 ± 58.2	3.7 ± 0.3
C	159.7 ± 2.2	8.2 ± 1.3
S	185.5 ± 6.5	4.7 ± 0.1

Table 2. R_q of $Si_{ICP-RIE}$ after TMAH treatment measured with AFM.

R_q of sidewalls, nm	Min in TMAH 25%, min	R_q after TMAH treatment, nm
217.2 ± 6.7	2	127.0 ± 8.0
157.0 ± 3.0	5	104.0 ± 3.5
241.7 ± 58.2	5	109.0 ± 5.0
159.7 ± 2.2	10	145.3 ± 5.0

2.2. Metalorganic Chemical Vapor Deposition of AlN Thin Films on Si (111) Vertical Surfaces

Figure 2 shows a cross-section scanning electron microscopy (SEM) image of nominally 1 µm thick AlN film deposited on 200 µm deep Si_{TMAH}. At the top of the cavity, AlN film thickness on the vertical sidewall is equal to the targeted film thickness. However, the film thickness decreases down the vertical sidewall. This is most likely due to the limited diffusion of reactant species into the cavities during the MOCVD growth process of AlN.[16] The same thickness gradient of 4 nm μm^{-1} was measured on AlN deposited on both Si_{TMAH}. and $Si_{ICP-RIE}$. However, the thickness gradient was non-linear in some areas on the sidewall, as shown in Figure 2.

Figure 3 shows SEM micrographs of AlN films deposited on b,c) $Si_{ICP-RIE}$ and d,e) Si_{TMAH}. As can be seen, both films have uniform coverage over the sidewall. AlN film deposited on $Si_{ICP-RIE}$ has a more pronounced mosaic structure (Figure 3b). Figure 3d shows defects in AlN deposited on Si_{TMAH}.

Figure 4 shows AFM and SEM images of a,b) pinholes and c,d) surface blisters observed on the AlN films deposited on Si_{TMAH}. The pinholes were localized mainly in the upper part of the cavity, while the blister-rich regions were concentrated closer to the cavity bottom and showed round shapes of foreign material in the AlN film. Energy dispersive X-ray (EDX) composition analysis in SEM revealed that Al content inside the blisters is higher than in the rest of the film, indicating Al-inclusions or droplets. Si etch-pits formed during TMAH etching can act as attraction centers for defect formation. Also, from the literature,[17] the formation of Al-rich regions may be provoked by the low mobility of Al adatoms. Thus, the formation of Al-rich regions might be due to the low diffusion rate of Al atoms at the bottom of the cavity. However, such a theory does not justify why Al blisters were not observed in the films deposited on sidewalls formed by ICP-RIE etching. Most probably, the formation of defect regions is due to a combination of several factors and thorough research should be conducted to investigate its origin.

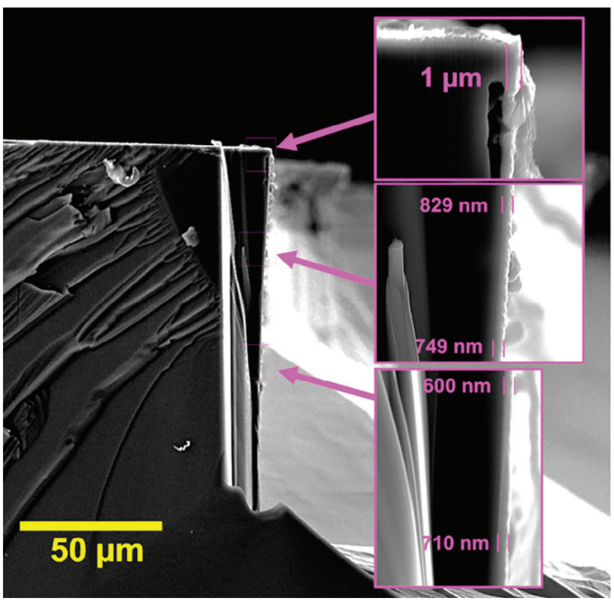

Figure 2. SEM micrographs of the cross-section of the vertical Si (111) sidewall with MOCVD AlN thin film on the wall.

The microstructure of AlN films deposited on $Si_{ICP-RIE}$ and Si_{TMAH} is shown in the bright field scanning transmission electron microscopy (BF-STEM) micrographs in **Figure 5**. Both films have columnar structure characteristic of mosaic polycrystalline AlN with preferred c-axis orientation. In both cases the films have grains height and size spread. For AlN deposited on Si_{TMAH} the grain size is in the range from 0.93 to 1.13 µm, while the grain size of AlN deposited on $Si_{ICP-RIE}$ is smaller (0.61 – 0.93 µm). Moreover, the STEM-BF images in Figure 5a show that AlN grows over the voids in Si for the sample where vertical sidewalls were formed in TMAH. The voids are most probably related to the etching pits formed during TMAH etching as discussed earlier. A closer inspection of the AlN/Si interfaces of both AlN on Si_{TMAH} and $Si_{ICP-RIE}$ is demonstrated in high resolution transmission electron microscopy (HRTEM) images in **Figure 6**. In Figure 6a a thin layer on the top of the Si voids can be seen. Etching pits in Si were likely filled by Si during annealing with disilane in the MOCVD reactor. During lamella preparation, thin Si layer and bulk Si were milled at different rates, leaving the empty areas in the lamella. No gaps or voids were found on the AlN/Si interface for the sample where AlN was deposited on $Si_{ICP-RIE}$.

The orientation and crystalline structure of AlN films are further verified by selected area electron diffraction (SAED) patterns shown in **Figure 7**. SAED patterns of the AlN films indicate that the films have crystallized with a preferred orientation in [0001] direction. The film deposited on Si_{TMAH} shows a high degree of crystallinity and uniform alignment of AlN (0002) with Si (111) (AlN(0002)||Si(111)). For the AlN deposited on $Si_{ICP-RIE}$, the AlN (0002) reflections are not completely aligned with the Si (111), indicating tilt of AlN grains in respect to Si.

Thus, when AlN grows on the smooth vertical Si surfaces, e.g., those formed using TMAH, the c-axis of AlN grains are perpendicular to the substrate's surface and well-aligned with each other, as schematically shown in **Figure 8a**. The film covers the vertical sidewalls uniformly and AlN grains grow perpendicular to the surface of the substrate in its every location in the case of high surface roughness as well. This can be seen in a wider-area BF-STEM micrograph in Figure 8c. SAED shows some grain tilt of AlN around [0001] direction, but the origin of the tilt is likely the Si surface quality, not the misorientation of the AlN grains in general. Thus, the growth of AlN films and AlN film crystalline orientation is following the vertical sidewall surface normal rather than crystallographic orientation of the substrate. Similar growth mechanism was demonstrated previously for sputter-deposited AlN when the film was grown on the amorphous substrate.[18]

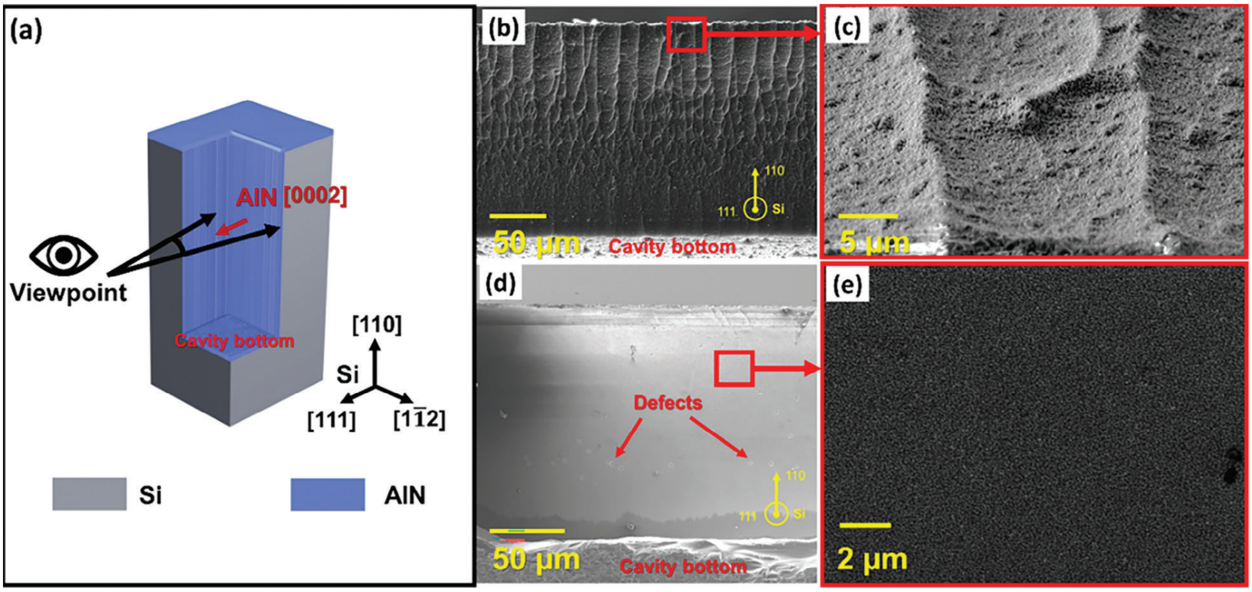

Figure 3. a) Schematic illustration of the structure under study; SEM micrographs of AlN films deposited on: b,c) $Si_{ICP\text{-}RIE}$, d,e) Si_{TMAH}.

3. Conclusion

AlN thin films were deposited on vertical Si (111) surfaces of the patterned Si (110) wafers that were etched using ICP-RIE and TMAH. In both cases MOCVD AlN films demonstrated full sidewall coverage and grew crystalline in c-axis direction. $Si_{ICP\text{-}RIE}$ and Si_{TMAH} showed large differences in sidewall R_q, and wet etched surfaces displayed significantly smoother surfaces. The R_q had a large effect on the crystallinity and orientation of the grown AlN films. AlN films grown on Si_{TMAH} were highly crystalline and oriented in [0001] direction, while the films grown on $Si_{ICP\text{-}RIE}$ displayed a lower level of alignment with the Si

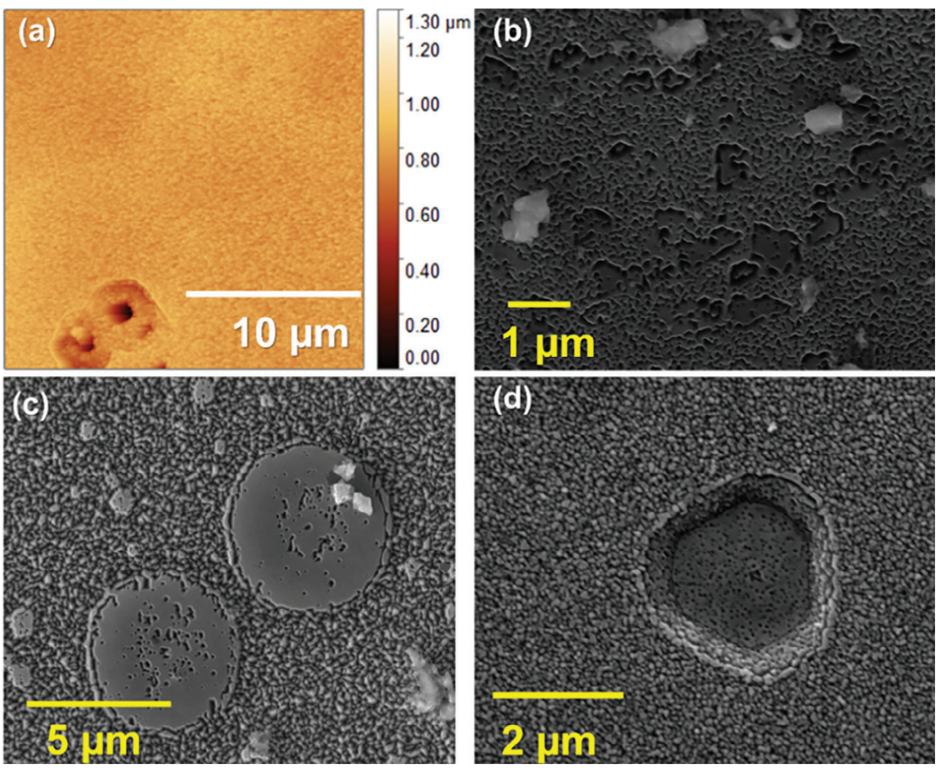

Figure 4. Defects in AlN films deposited on the Si_{TMAH}. a) AFM scan of the pinholes and misoriented grains around the pinholes; SEM micrographs of the b) pinholes; c,d) Al-rich droplets.

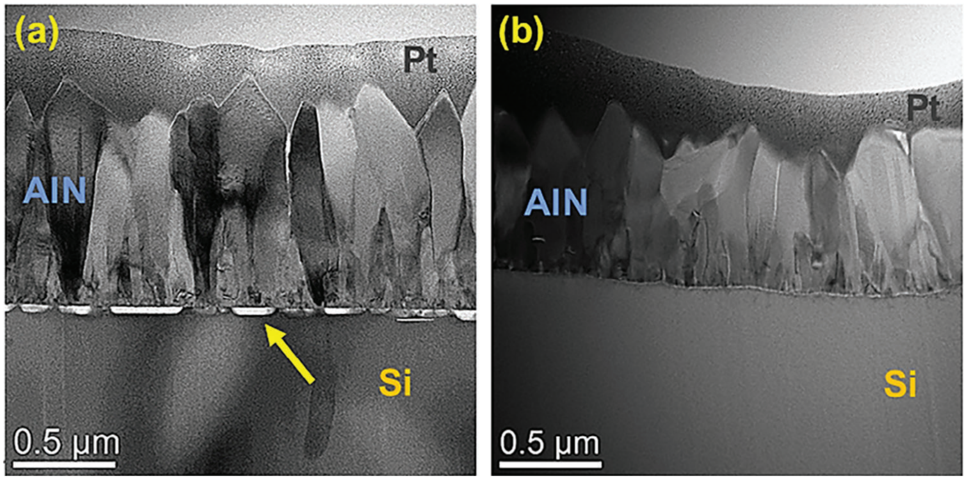

Figure 5. BF-STEM micrographs of AlN films on vertical surface obtained using a) TMAH; b) ICP-RIE. The yellow arrow here is pointing the location of the etching pit at the AlN/Si interface.

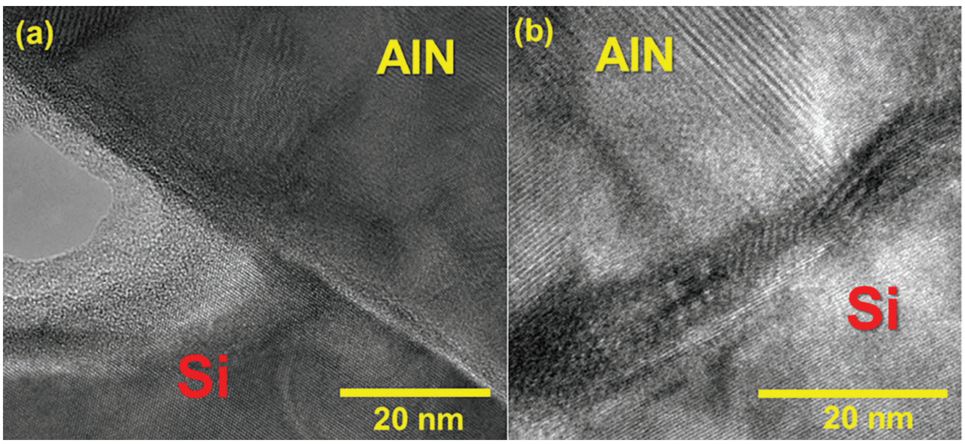

Figure 6. HRTEM micrographs of AlN films on a) Si_{TMAH}, and b) $Si_{ICP\text{-}RIE}$.

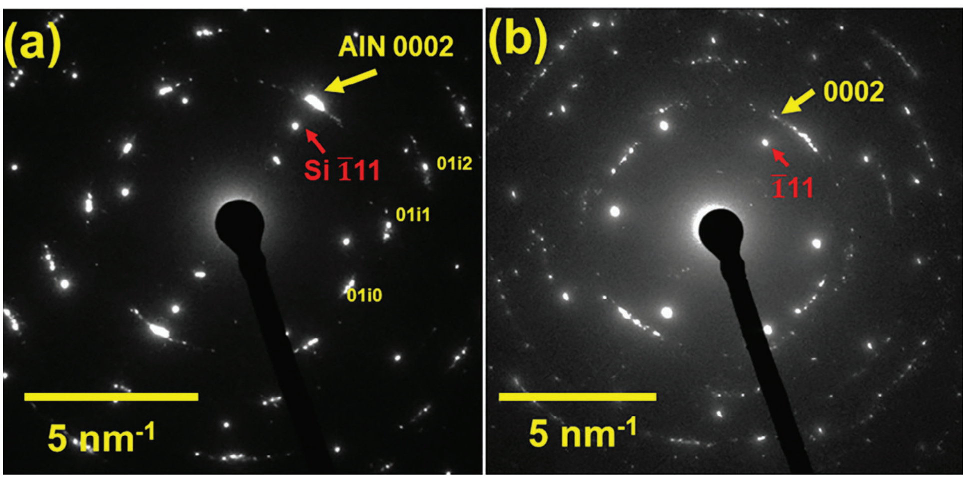

Figure 7. SAED patterns of the AlN film on a) Si_{TMAH}, and b) $Si_{ICP\text{-}RIE}$.

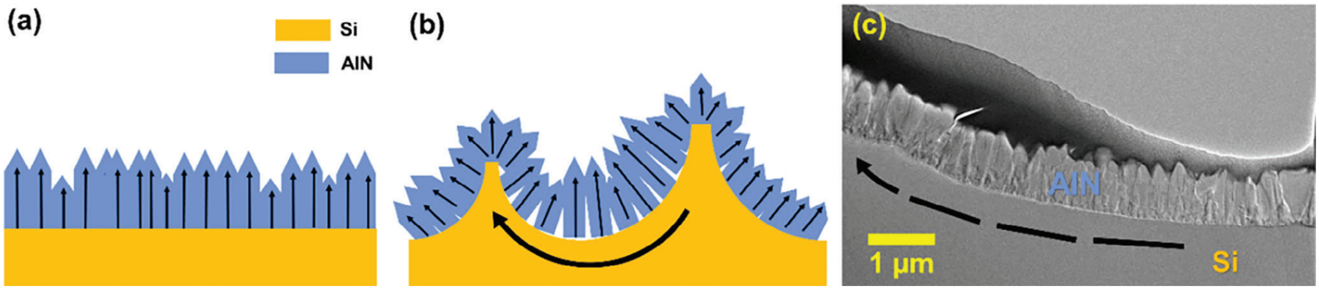

Figure 8. Schematic illustration of AlN thin film growth on a) Si_{TMAH}; b) $Si_{ICP-RIE}$. Black arrows indicate the direction of c-axis orientation in AlN grains. c) BF-STEM micrograph of AlN deposited on $Si_{ICP-RIE}$.

sidewalls. While exhibiting smoother surface morphology, AlN films deposited on Si_{TMAH} had pronounced density of defects: pinholes and Al-rich regions. Further extensive research is needed to determine the root cause of the defects formation. In addition, vertical Si surfaces treatment by TMAH was tested for reduction of R_q of the vertical walls in patterned Si. The capacity of this method is limited, and it cannot be used for surface roughness smoothening of surfaces with high R_q value. Ultimately, when grown on low surface roughness, high crystal quality AlN can be achieved for MEMS applications . AlN on high roughness surfaces grows in c-axis direction but is expected to demonstrate an overall lower piezoelectric response when compared to AlN grown on a smoother surface. Highly oriented AlN likely might be achieved when grown on $Si_{ICP-RIE}$ if the etching process is optimized so that the R_q value of the sidewalls is comparable to the value of the vertical Si surfaces achieved by wet etching methods.

4. Experimental Section

Vertical Surface Preparation: Blank 100 mm Si (110) wafers were first thermally oxidized. A 1 µm thick silicon dioxide (SiO_2) layer was used as a hard mask thereafter. The hard mask was patterned with standard photolithography methods so that the cavity sidewalls were aligned with Si (111) orientation in Si (110). Windows in SiO_2 hard mask were etched using reactive ion etching (RIE). Cavities with Si (111) vertical sidewalls were etched using wet and dry etching. Si wet etching was conducted in tetramethylammonium hydroxide solution 25% (TMAH) at 70 °C. Dry etching was done using cryo-mode in ICP-RIE Plasmalab 100. For dry etching sulfur hexafluoride SF_6 (40 sccm) and oxygen O_2 (6 sccm) gas mixture was used. The etching was conducted at −110 °C. The hard mask was subsequently removed in HF. The process of cavities formation in Si (110) is shown in **Figure 9**.

MOCVD of AlN Films: AlN films were deposited on patterned and blank substrates using Aixtron 1 × 4″ close-coupled showerhead MOCVD reactor. First, the wafer was annealed for 5 min in hydrogen (H_2) and ten more minutes in disilane (Si_2H_6) at 1025 °C and 300 mbar reactor pressure. Surface nitridation was done under an ammonia (NH_3) atmosphere for 15 s at 980 °C and 100 mbar reactor pressure.

AlN was grown with a two-step growth process. First, a low-temperature buffer layer was deposited at 980 °C, followed by deposition of 1 µm AlN layer at 1085 °C. During AlN growth, H_2 was used as a carrier gas and trimethylaluminium (TMAl) and ammonia (NH_3) were used as precursors for aluminum and nitrogen, respectively. AlN film crystalline quality and surface roughness were optimized by growing test samples on planar Si (111) wafers with varying pressure and V/III ratio. The optimal growth parameters (100 mbar, V/III 336) were used for AlN deposition on the Si (111) vertical sidewalls of the patterned Si (110) wafers.

The films have *c*-axis orientation when grown on blank Si (111). No other than (0001)-family reflections are captured in a symmetrical $2\theta - \omega$ scan implemented using high-resolution X-ray diffraction (HRXRD). The full width at half maximum (FWHM) value of the X-ray rocking curve (XRC) around (0002) reflection is 0.61°.

The positioning of AlN on the sidewalls and its crystalline orientation with respect to Si are illustrated in **Figure 10a**.

Characterization Methods: HRXRD measurements (Rigaku Smart lab) were used to assess the crystalline quality of the AlN films deposited on blank Si (111) wafers. XRC scan around AlN (0002) reflection was recorded, and the FWHM of the (0002) reflection was measured. The surface morphology of AlN films was studied using a scanning electron microscope (SEM). AlN thin film thickness deposited on the blank Si

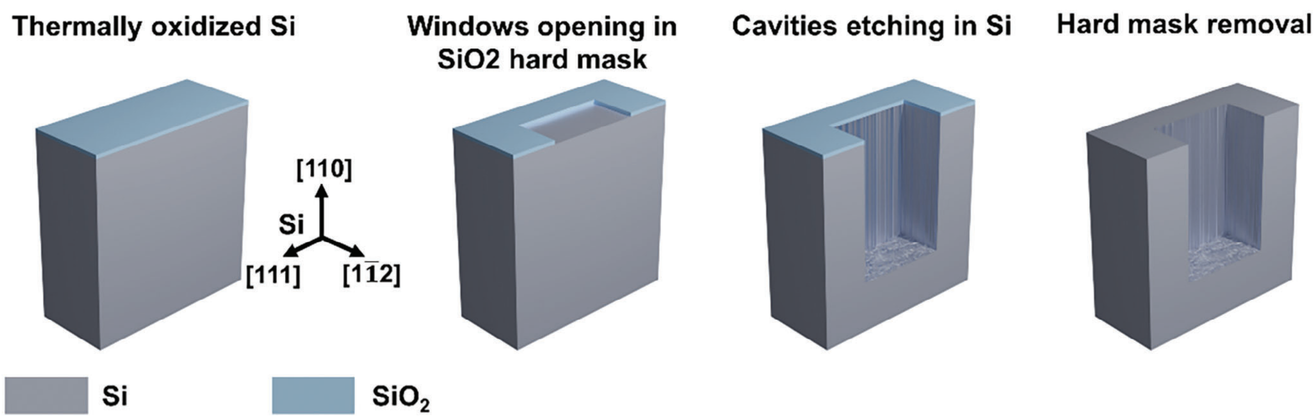

Figure 9. Process of cavities formation in Si (110).

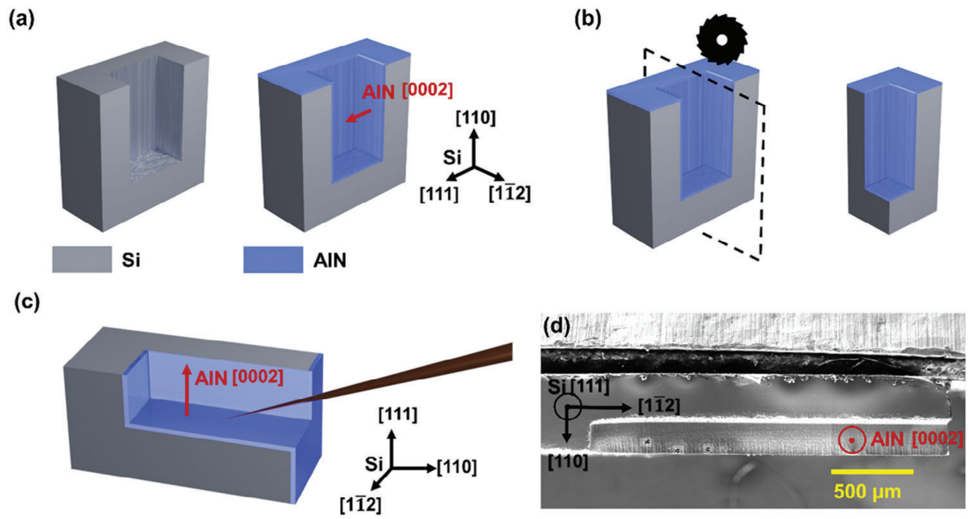

Figure 10. a) Schematic illustration of AlN deposited on the vertical sidewalls in Si; Schematic illustration of the b) sample's dicing and c) lamella preparation;d) SEM micrograph of the sample ready for the lamella extraction.

(111) wafers was measured using a spectroscopic ellipsometer Semilab SE-2000.

The cavities in the patterned Si (110) wafers were diced using a dicing saw, as shown in Figure 10b. The cut was made in the center of the cavity, thus allowing access to the vertical sidewalls for AFM and transmission electron microscopy (TEM) lamella preparation when the sample is mounted at 90°, as shown in Figure 10c,d. AFM Bruker Dimension Icon was used to measure the surface roughness of the vertical sidewalls and the deposited AlN thin films. Every wafer was measured in five different locations, designated by the first letters of the cardinal points. RMS R_q of the vertical surfaces is an average of three cavities on the same wafer. In addition, the impact of the post-dry etching TMAH treatment on the R_q of the vertical Si (111) surfaces in Si (110) was studied. For that, samples were etched in ICP-RIE for 60 min and surface roughness of the formed sidewalls was measured in AFM. After, the samples were dipped in TMAH 25% (70 °C) solution for 2, 5, and 10 min. R_q of the samples was measured repeatedly after TMAH treatment.

The microstructure of the AlN films deposited on vertical surfaces and the orientation relationship between the AlN film and the vertical Si (111) planes were investigated using TEM. Lamellas of AlN films on vertical sidewalls were prepared using JEOL JIB-4700F. The lamellas were investigated under a high-resolution TEM (HRTEM) JEOL JEM-2200FS with a 200 kV acceleration voltage. Both BF-STEM micrographs and SAED were recorded. SAED were recorded along the Si [110] zone axis. The thickness uniformity of the AlN films on Si (111) vertical sidewalls in Si (110) was measured in SEM. The sample was cleaved and ion-polished along the vertical sidewall using a focused ion beam (FIB) to make a cross-section of the cavity. The thickness of AlN was measured along the vertical wall of the cavity.

Acknowledgements

This work has been carried out as part of ECSEL18 Project NewControl, which receives funding within the Electronic Components and Systems for European Leadership Joint Undertaking (ESCEL JU) in collaboration with the European Union's Horizon2020 Framework Programme and National Authorities, under grant agreement №. 826653-2. The authors would like to acknowledge the Innovation Funding Agency Business Finland for their financial support. The authors acknowledge the provision of facilities and technical support of Aalto University at OtaNano Nanomicroscopy Center (Aalto-NMC). K.B. acknowledges support from the HPY Research Foundation, Foundation of Electronics Engineers (Elektroniikkainsinöörien Säätiö), and Walter Ahlström foundation.

Conflict of Interest

The authors declare no conflict of interest.

Data Availability Statement

The data that support the findings of this study are available from the corresponding author upon reasonable request.

Keywords

aluminum nitride (AlN), MOCVD, surface roughness, thin film, vertical sidewall

Received: September 14, 2023
Revised: January 4, 2024
Published online:

[1] K. Bespalova, T. Nieminen, A. Gabrelian, G. Ross, M. Paulasto-Kröckel, *Adv. Electron. Mater.* **2023**, *9*, 2300015.
[2] A. Gabrelian, G. Ross, K. Bespalova, M. Paulasto-Kröckel, *Mater. Today Commun.* **2022**, *33*, 104522.
[3] E. Österlund, S. Suihkonen, G. Ross, A. Torkkeli, H. Kuisma, M. Paulasto-Kröckel, *J. Cryst. Growth* **2020**, *531*, 125345.
[4] E. Österlund, H. Seppänen, K. Bespalova, V. Miikkulainen, M. Paulasto-Kröckel, *J. Vac. Sci. Technol., A* **2021**, *39*, 032403.
[5] M. Ramezani, V. V. Felmetsger, N. G. Rudawski, R. Tabrizian, *IEEE Transactions on Ultrasonics, Ferroelectrics, and Frequency Control* **2020**, *68*, 753.
[6] K. Tonisch, V. Cimalla, C. Foerster, D. Dontsov, O. Ambacher, *physica status solidi* **2006**, *3*, 2274.
[7] C.-B. Eom, S. Trolier-Mckinstry, *MRS Bull.* **2012**, *37*, 1007.
[8] L. Huang, Y. Li, W. Wang, X. Li, Y. Zheng, H. Wang, Z. Zhang, G. Li, *Appl. Surf. Sci.* **2018**, *435*, 163.
[9] M. Zalazar, P. Gurman, J. Park, D. Kim, S. Hong, L. Stan, R. Divan, D. Czaplewski, O. Auciello, *Appl. Phys. Lett.* **2013**, *102*, 104101.
[10] S. M. Curtis, N. Wolff, D. Dengiz, H. Lewitz, J. Jetter, L. Bumke, P. Hayes, E. Yarar, L. Thormählen, L. Kienle, D. Meyners, E. Quandt, *J. Mater. Res.* **2020**, *35*, 1298.

[11] G. Ross, H. Dong, C. B. Karuthedath, A. T. Sebastian, T. Pensala, M. Paulasto-Kröckel, *Mater. Des.* **2020**, *2020196*, 109126.
[12] K. Biswas, S. Kal, *Microelectron. J.* **2006**, *37*, 519.
[13] D. Iencinella, E. Centurioni, R. Rizzoli, F. Zignani, *Sol. Energy Mater. Sol. Cells* **2005**, *87*, 725.
[14] M. A. Gosálvez, I. Zubel, E. Viinikka, in *Handbook of Silicon Based MEMS Materials and Technologies*, (Eds: V. Lindroos, M. Tilli, A. Lehto, T. Motooka), William Andrew Publishing, USA **2009**, 24.
[15] M. A. Gosálvez, K. Sato, A. S. Foster, R. M. Nieminen, H. Tanaka, *J. Micromech. Microeng.* **2007**, *17*, S1.
[16] S. Suihkonen, M. Ali, O. Svensk, S. Sintonen, M. Sopanen, H. Lipsanen, P. T. Törmä, V. Nevedomsky, N. Bert, *physica status solidi* **2011**, *8*, 1509.
[17] P. Shao, S. Li, Z. Li, H. Zhou, D. Zhang, T. Tao, Y. Yan, Z. Xie, K. Wang, D. Chen, B. Liu, Y. Zheng, R. Zhang, T. Lin, L. Wang, H. Hirayama, *J. Phys. D: Appl. Phys.* **2022**, *55*, 364002.
[18] A. Artieda, M. Barbieri, C. S. Sandu, P. Muralt, *J. Appl. Phys.* **2009**, *105*, 024504.